AD_____

Award Number: DAMD17-02-1-0613

TITLE: Optical Imaging of Mammaglobin Expression in Breast Cancer

PRINCIPAL INVESTIGATOR: Samuel Achilefu, Ph.D.

CONTRACTING ORGANIZATION: Washington University
St. Louis, Missouri 63110

REPORT DATE: May 2004

TYPE OF REPORT: Annual

PREPARED FOR: U.S. Army Medical Research and Materiel Command
Fort Detrick, Maryland 21702-5012

DISTRIBUTION STATEMENT: Approved for Public Release;
Distribution Unlimited

The views, opinions and/or findings contained in this report are those of the author(s) and should not be construed as an official Department of the Army position, policy or decision unless so designated by other documentation.

REPORT DOCUMENTATION PAGE

Form Approved
OMB No. 074-0188

1. AGENCY USE ONLY (Leave blank)	2. REPORT DATE	3. REPORT TYPE AND DATES COVERED
	May 2004	Annual (1 May 2003 - 30 Apr 2004)

4. TITLE AND SUBTITLE
Optical Imaging of Mammaglobin Expression in Breast Cancer

5. FUNDING NUMBERS
DAMD17-02-1-0613

6. AUTHOR(S)
Samuel Achilefu, Ph.D.

7. PERFORMING ORGANIZATION NAME(S) AND ADDRESS(ES)
Washington University
St. Louis, Missouri 63110

E-Mail: achilefus@wustl.edu

8. PERFORMING ORGANIZATION REPORT NUMBER

9. SPONSORING / MONITORING AGENCY NAME(S) AND ADDRESS(ES)
U.S. Army Medical Research and Materiel Command
Fort Detrick, Maryland 21702-5012

10. SPONSORING / MONITORING AGENCY REPORT NUMBER

11. SUPPLEMENTARY NOTES
Original contains color plates: All DTIC reproductions will be in black and white.

12a. DISTRIBUTION / AVAILABILITY STATEMENT
Approved for Public Release; Distribution Unlimited

12b. DISTRIBUTION CODE

13. ABSTRACT (Maximum 200 Words)

Mammaglobin (MMG) is a breast-specific glycoprotein that is over-expressed in nearly 80% of primary and metastatic breast cancers. The exact biological function of this secreted protein is not known. An important step towards understanding the role of MMG in breast carcinogenesis is to monitor its expression in MMG-expressing tumors. This step could be accomplished by labeling antibodies directed to MMG with radioactive or fluorescent antennas. To evaluate the presence of putative MMG receptors, we also labeled the protein and the truncated peptide analogues with radioactive and fluorescent probes, which were injected in tumor-bearing rodents. We successfully prepared and labeled 4 truncated MMG peptide analogues with near infrared and radioactive probes. In vitro MTT assay shows that one of these compounds is not cytotoxic and do not induce cell proliferation. The in vivo imaging studies by fluorescent imaging and positron emission tomography show similar biodistribution of the probes in the liver and kidneys of nude mice. The fluorescently-labeled anti-MMG antibodies are selectively retained in the target tumor tissue and also the major excretion organs, liver and kidneys.

14. SUBJECT TERMS
Optical imaging, optical contrast agents, radiopharmaceuticals, positron emission tomography, mammaglobin, breast cancer

15. NUMBER OF PAGES
36

16. PRICE CODE

17. SECURITY CLASSIFICATION OF REPORT	18. SECURITY CLASSIFICATION OF THIS PAGE	19. SECURITY CLASSIFICATION OF ABSTRACT	20. LIMITATION OF ABSTRACT
Unclassified	Unclassified	Unclassified	Unlimited

Table of Contents

INTRODUCTION

Mammaglobin (MMG) expression is uniquely associated with human breast and, more importantly, it is up-regulated in breast cancer. Therefore, targeting MMG expression in vivo provides an opportunity to develop a novel approach to image breast cancer. This concept is based on the premise that the concentration of secreted MMG will be up-regulated in the tumor-microenvironment, thereby facilitating the localization of breast cancer and possible metastasis. This will require the use of highly sensitive methods that can detect low levels of diagnostic protein expressions in vivo. This criterion can be satisfied by the use of optical or nuclear imaging method. Therefore, this project focuses on preparing anti-MMG antibodies, native glycosylated MMG protein, and non-glycosylated synthetic MMG, labeling the biomolecules with optical or nuclear probes, and evaluating the possibility of localizing tumors by either or both of these methods. We have successfully prepared novel molecular probes that are directed to MMG and anti MMG antibodies. All the MMG-related peptides and antibodies prepared are non-cytotoxic at the low micromolar concentration range that is useful for in vivo imaging. Preliminary data suggest that targeting the local concentration of MMG in breast cancer is a more useful strategy to image MMG expression than directing the probes to putative MMG receptors. We are on track to accomplish all the tasks approved for the entire funding period. The complete results will be presented at the Era of Hope meeting in Philadelphia, 2005.

BODY OF REPORT

As described in our approved Statement of Work, the scope of this project requires that several components of the work run concurrently. Integrating most components of the project has enabled us to channel our resources to potentially high impact aspects of the study. The following activities were approved for this report period:

TASK 1

Synthesis and labeling studies (Months 1-30)

We are on track to complete the synthesis of all the compounds proposed in the Award. Synthesis of the remaining compounds will be completed by the end of the funding period, as proposed.

TASK 1(a)

Synthesize and characterize two mouse anti-mammaglobin monoclonal antibodies (AMABs) conjugates of cypate, a near infrared indotricarbocyanine optical probe (cypate).

In our last report, we disclosed the successful synthesis of the optical probes needed for this study with improved yields. Part of this study is now published in the American Chemical Society Journal *Organic Letters,*[1] and the Proceedings of the SPIE.[2] An invited review article has been accepted for publication in *Current Medicinal Chemistry*[3] and another invited review manuscript is under consideration by the editor of the journal *Technology in Cancer Research & Treatment.*[4] Because of the large size of the manuscript, copies of the review papers will be sent to US Army Medical Research and Materiel Command once the pre-prints become available.

Although the newly anti MMG antibody-based near infrared molecular beacons have been presented at scientific meetings, we are awaiting the completion of the imaging studies before submitting a comprehensive manuscript on these multidisciplinary studies.

TASK 1(b)

Label mouse AMAB with ^{111}In and ^{64}Cu chelates; purify and characterize radiolabeled AMAB.

As indicated in the previous report, labeling of the anti MMG antibodies with radioactive ^{64}Cu was successful and the compounds were used for in vivo biodistribution studies.

TASK 1(c)

Synthesize native MMG glycoprotein in bacteria and non-glycosylated synthetic MMG proteins by segment-condensation peptide synthesis; label with optical and radioactive probes.

(i) **Preparation of bacterially expressed MMG:** We accomplished this Task in Year 1 of the project and we are now scaling up the production to enable us to label and purify sufficient amounts of products for in vitro and in vivo evaluation of MMG.

(ii) **Preparation of non-glycosylated synthetic MMG:** In the last report, we disclosed our intention to synthesize four MMG peptide fractions, which are shown below:

MKLLMVLMLAALSQHCYA
GSGCPLLENVISKTINPQVSKTEYKELLQEF
IDDNATTNAIDELKECF
LNQTDETLSNVEVFMQLIYDSSLCDLF

Synthesis of these peptides became a major challenge because of the formation of tertiary structures that inhibited the coupling of subsequent amino acids. After several attempts, this reaction was finally successful when we redesigned the fragmentation pattern to take into account the presence of cysteine residues that can cross-link the peptides by intermolecular disulfide oxidation. Consequently,

the following structures became the target of our new strategy to prepare MMG peptide fragments:

MMG1: **MKLLMVLMLAALSQHCYA**GSG
MMG2: **CPLLENVISKTINPQVSK**
MMG3: **TEYKELLQEFIDDNATTNA**
MMG4: **IDELKECFLNQTDETLSNVEVFMQLIYDSSLCDLF**

The cysteine residue in MMG1 was replaced with ethyl-protected cysteine amino acid [Cys(Et)-OH] to avoid the liberation of free thiol group. Because conjugation of near infrared probe or DOTA will occur at the amino terminus of the peptides, no additional protection of the cysteine residue in MMG2 was needed. The steric hindrance provided by cypate or DOTA chelating group will minimize deleterious effects of the free thiol group. MMG3 has no cysteine amino acid residue and it is expected to retain the functional status of this MMG motif. MMG4 is designed to have two cysteine amino acid residues in the same fragment so that we can induce intramolecular cyclization to prevent polymerization due to cross-linkages. We are using a method we reported previously in the literature to accomplish this particular synthesis.[5,6]

Procedure: The first amino acid was loaded on the resin at < 0.4 mmol/g. The peptides were prepared with ACT APEX 396 peptide synthesizer by standard Fmoc protocol,[7] as described previously.[5,8] A Wang resin pre-loaded with the first amino acid on a 30-μmole scale was placed in a reaction vessel. Subsequent Fmoc-protected amino acids were sequentially coupled to the resin-bound amino acid from the carboxyl to amino terminus. Fmoc removal was performed with 20% piperidine in dimethyl formamide (DMF). The coupling reagents N-hydroxybenzotriazole (HOBt) and 2-(1H-benzotriazol-1-yl)-1,1,3,3-tetramethyl uronium hexafluoro phosphate (HBTU) were used for the peptide synthesis. Peptide cleavage and concomitant removal of the amino acid side chain protecting groups were accomplished with TFA (85%), distilled water (5%), phenol (5%),

and thioanisole (5%). The crude peptide was precipitated in cold *t*-butyl methyl ether (MTBE) and lyophilized in acetonitrile/water (2:3) mixture. The resulting powder was purified by HPLC and analyzed by mass spectrometry and analytical HPLC.

Conjugation of near infrared probe (cypate) or chelating group (DOTA) with the peptides: We successfully labeled the MMG peptide fragments with the metal chelating group (DOTA) and with the near infrared probe (cypate) by solid phase synthesis. This approach enabled us to obtain the desired compounds in high purity (>95%, HPLC) for in vitro and in vivo studies. Typically, the peptide was synthesized on solid support as described above and the N-terminal Fmoc was removed with 20% piperidine in DMF. Cypate or tri-*t*-butyl DOTA was pre-activated with diisopropyl carbodiimide (DIC) and added to the peptide on solid support. After 8 h, the peptide conjugate was cleaved from the resin, as described above, and the product was purified by HPLC.

Thus, we have successfully prepared MMG peptide fragments that are useful for throughput screening of putative MMG receptor in MMG-producing breast tumors.

TASK 1(d)

Identify the peptide motifs that bind to MMG.

We used five rounds of phage display reiterations to thoroughly screen and identify peptides that bind to MMG. The following peptide sequences were consistently identified by this method:

GAPNKAHD
VGLVAK
LQRGR
GLSRAWEVDF
RGRLQ
MHQSG
VTPFA

We are now in the process of validating this observation by ELISA binding assays and Western blot. Fluorescent and radioactive probe conjugates of these peptides will be prepared within the next 6 months and evaluated in MMG-positive breast tumors.

TASK 1(e)

Prepare the identify AMAB peptide sequence in each antigen-binding site and synthesize MMG peptide mimics.

Monoclonal antibodies have been developed to the MMG protein[9] and we are using these reagents for our detection experiments. These monoclonal antibodies recognize the native MMG protein complex and have been used to develop an ELISA assay to detect MMG in sera and tissues. This information provides supporting data that the labeled MMG antibodies will be ideal tools for the optical detection of MMG positive breast cancer cells.

Our in vivo biodistribution studies in MD 361 tumor bearing mice identified MMG2 and MMG3 as good candidates to optimize the binding of MMG to its putative receptors. We are currently evaluating the recognition of these polypeptides with antibodies directed against MMG.

TASK 1(f)

Optimize MMG binding affinity by semi-combinatorial approach and identify four peptides with high MMG binding affinity and specificity.

We have identified and synthesized seven different peptides that bind MMG (see Task 1d above). Using these as templates, we are scaling up their synthesis and all compounds will be labeled with cypate or DOTA for biological screening. We anticipate completing the synthesis and labeling within the next 6 months.

TASK 1(g)

Label the identified four MMG-avid peptides with a near infrared optical probe and radioactive metal chelates; purify and characterize the final compounds.

This work is in progress (see Task 1f above) and within the time line described in the grant proposal.

TASK 2

In vitro biological assays of mammaglobin-specific contrast agents (Months 6-30).

We used MTT assay to evaluate the proliferative and cytotoxic effects of MMG and its analogues. Cells incubated with MMG began to show signs of cytotoxicity in the micromolar concentration range while the truncated MMG peptide analogue MMG2 is not cytotoxic and do not induce cell proliferation. However, the MTT assay suggests that MMG 3 induces concentration-independent cell proliferation. We also constructed a novel hybrid of MMG with the cell internalizing peptide, Tat-peptide. Western blots were used to evaluate the affinity of peptides towards MMG on MD 361 cells. The ensemble of these results demonstrates the feasibility of developing contrast agents for MMG detection. Additionally, we are in the process of developing a stably transfected MMG-green fluorescent protein (MMG-GFP) cells that will allow us to track the migration and distribution patterns of MMG in female nude mice.

TASK 2(a)

Characterize and classify six cell lines as MMG-positive and MMG-negative cancer cells. These include four human breast cancer cell lines, MDA-MB-415, MDA-MB-361, MDA-MB-451, and MCF-7, and two established rat acinar pancreatic cell lines, CA20948 and AR42-J.

In our previous report, we identified MDA-MB-415 and MDA-MB-361 as MMG-positive breast cancer cell lines. We also established that CA20948 and, subsequently, AR42-J cells are MMG-negative. These results enabled us to choose MDA-MB-361 and CA20948 for positive and negative controls in our studies. Unfortunately, the MDA-MB-361 and MDA-MB-415 grow very slowly in nude mice. Switching from male to female nude mice and subsequent implantation of the tumor cells in the mammary pad of female nude mice did not enhance tumor development. This problem has limited the progress of our study. Consequently, we recently identified a different MMG-expressing breast tumor cell line, ZR-75-1. This cell line is commercially available from ATCC. It is both estrogen and progesterone receptor-positive cell line used for in vitro and animal studies.[10-12] We plan to substitute MD-MB-361 with ZR-75-1 to accelerate our imaging studies.

TASK 2(b)

Label MMG-positive human breast cancer cells with Zynaxis dye and assess by fluorescence microscopy the existence of MMG breast cancer receptor and preferential retention of the heavily glycosylated MMG proteins in pathologic cells due to intimate association or strong adhesion of MMG to cancer cells.

This study is in progress using MDA-MB-361. Because our microscopes are not equipped to operate in the near infrared wavelengths, we had to prepared new optical probes that can be used with standard microscopes. Consequently, we have successfully completed the synthesis of fluorescent probes that absorb in the visible wavelengths for microscopy and their conjugation to peptides and proteins is in progress.

TASK 2(c)

Label MMG-positive human breast cancer cells with Zynaxis dye and determine by fluorescence microscopy the retention and specificity of MMG and AMAB peptide mimics in a mixture of labeled MMG-positive and unlabeled MMG-negative cells; identify possible fluorescence phase shift and polarization changes between bound and unbound MMG.

For the same reason stated in 2b above, this study is in progress using MDA-MB-361 cells.

TASK 2(d)

Evaluate the internalization of AMAB, AMAB peptide mimics, synthetic MMG protein, and native MMG glycoprotein in breast caner cells to probe cytoplasmic MMG. If self-internalization is not feasible, investigate the use of Tat-peptides as adjuvant internalization agents.

We slated this phase of the study towards the end of the project and we will tackle it in the final year of the study. One of the tasks described in the proposal is to use the Tat insertion motif for internalization and detection of MMG-positive cells. Accordingly, we have prepared and purified a Tat-MMG construct. The fusion protein was tested in dendritic cells as a method of antigen delivery for T-cell activation. This preliminary study indicates the feasibility of using Tat as an "insertion" motif to internalize MMG in cells. This work will be published in a scientific journal and funding from DoD will be acknowledged.

TASK 2(e)

Evaluate the effect of purified native MMG glycoprotein and synthetic MMG proteins on the proliferation of breast cancer cells in vitro.

Cell proliferation and cytotoxicity assays were performed using the 3-(4,5-dimethylthiazol-2-yl)-2,5-diphenyltetrazolium bromide (MTT)-based in vitro toxi-

cology assay kit (Sigma) per the manufacturer's protocol. Briefly, MDA-MB-361 cells were grown in 96 well plates to 75% confluence in phenol red-free Dulbecco's Modified Eagle's Medium supplemented with 10% fetal calf serum, 100 units/mL Penicillin G, 0.25 μg/mL Amphotericin B and 100 units/mL Streptomycin. The compound to be tested (0 – 125 μM) was added to each well in a final volume of 100 μL/well and the cells were incubated for 24 h at 37 °C in 5% CO_2. After incubation, the media was removed and replaced with 100 μL/well phenol red-free medium. Absorbance at 570 nm and 690 nm was measured. Ten microliters of MTT was added to each well and the cells were allowed to incubate for 2 h. The MTT solubilzation solution (100 μL of Formazan crystals dissolves in 0.04 N HCl in 2-propanol) was added to each well and formazan crystals were dissolved by vigorous pipetting. Absorbance at 570 nm and 690 nm was measured. The percent of viable cells *B* was determined according to the formula

$$B = \frac{(\lambda_{570} - \lambda_{690})_{treated}}{(\lambda_{570} - \lambda_{690})_{untreated}} \times 100,$$

where λ_{570} is the absorbance of formazan crystals at 570 nm and λ_{690} is background.

We first performed the assay with ethanol, which is an established cytotoxic agent to assure that the assay is working properly. As shown in Figure 1, nearly all the cells were no longer viable at about 30 min post-incubation. By using the same assay, we observed that native MMG was not cytotoxic up to 4 h post incubation. At 24 h, a linear decrease in cell viability was observed (Figure 1). However, we are encouraged that MMG is not cytotoxic and does not induce cell proliferation at the sub-micromole quantity we are using for in vivo studies, even after 24 h incubation period.

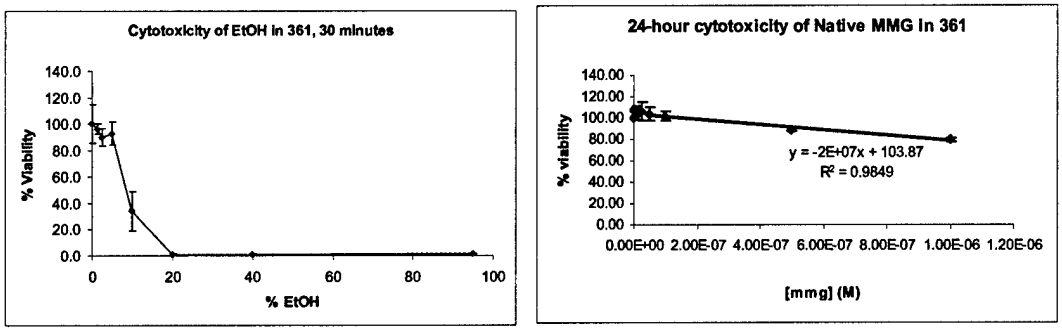

Figure 1: Cytotoxicity and cell proliferation assays for ethanol (left panel; concentration expressed as percentage of ethanol in phosphate buffer) and native MMG (right panel).

To the contrary, the synthetic peptide analogues MMG2 is apparently innocuous to cells up to 24 h at 1.0 µM and MMG3 induced cell proliferation that is not dependent on the peptide concentration (Figure 2). These data support the rationale to investigate further the development of peptide-based MMG molecular probes.

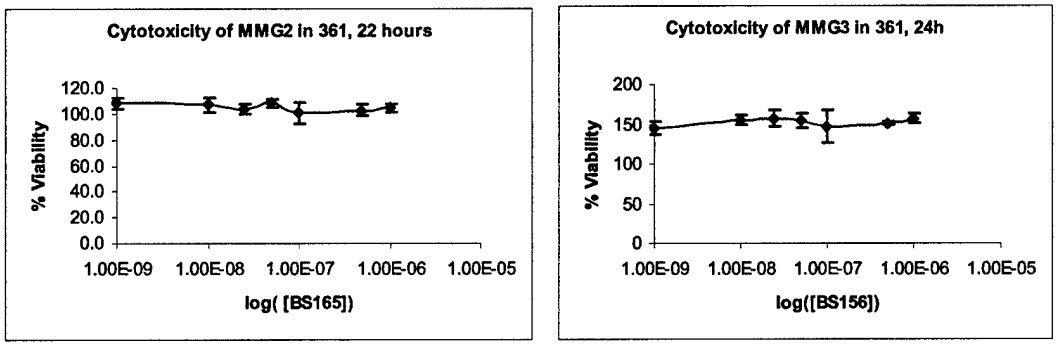

Figure 2: Cytotoxicity and cell proliferation assays for MMG2 (left panel) and native MMG (right panel).

TASK 2(f)

Develop competitive binding assays for MMG protein, AMAB and peptide mimics. Determine the binding affinity of optical and radiolabeled probes in breast cancer cell culture.

This section of the study will be performed in the final year of the Award. We have tested a peptide antibody, directed against the carboxy-terminal 18 amino acids of mammaglobin, and have demonstrated that this peptide antibody can bind to MMG. Importantly, the peptide can be used to successfully compete the

antibody, providing a working assay for testing other peptides relevant for mammaglobin binding (Figure 3).

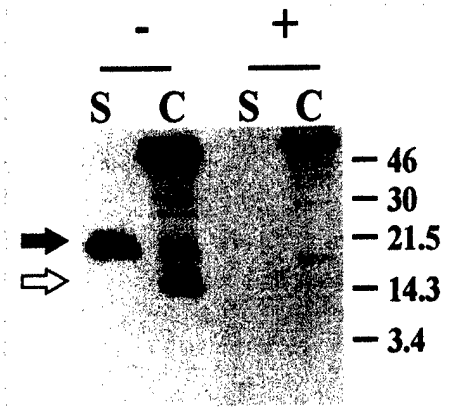

Figure 3: Detection of mammaglobin protein using a peptide antibody targeting mammaglobin. A ~21 kD band is detected by Western blot analysis in the culture supernatant (S) and a ~14 kD precursor form is observed in the cell lysate (C). The right panel (+) is identical to the left panel (-) except that competing carboxy peptide was added to demonstrate specificity of the peptide antibody generated to the mammaglobin protein. The gel was run under reducing conditions.

The experiments underway consist of MMG specific peptides, labeled with either DOTA or Cypate. The labeled peptides will be run on a 15% acrylamide gel with bacterially expressed MMG as the positive control. Using a polyclonal antibody derived from rabbits immunized with the bacterially expressed MMG, we will perform a Western blot to confirm that the anti-MMG antibody recognizes the peptides. Positive detection confirms that the labeled peptide still has antigenic detection since the antibody binding validates proper antigenic orientation. The results will be described in the final report.

TASK 3

Biodistribution and imaging of MMG-positive and MMG-negative tumor xenografts in rodents (Months 18-36).

Despite the limitations of our current tumor model (see Task 2a), we have continued to evaluate some of the molecular probes in tumor bearing and normal nude mice. The optical images we reported previously still represent the best contrast we have obtained so far. Although the in vivo imaging studies were

scheduled to start 18 months from the Award date, we started this earlier to facilitate integrating imaging information with in vitro studies. Below are the results of our imaging studies.

(i) **Optical Imaging of cypate-AMAB in mice:** A simple non-invasive *in vivo* continuous wave fluorescence imaging apparatus employed to assess the localization and distribution of contrast agents has been previously described.[8] Briefly, two de-focusing lenses were each placed in front of two laser diodes to expanded the beam such that the whole mouse was illuminated. The diodes emit radiation at 780 nm, which excites cypate conjugates. The lasers generated a nominal 50 mW of incident power but the power at the output of the bundle was approximately one-half of the input power. We used a Princeton Instruments CCD camera to capture the emitted light and an interference filter was placed in front of the CCD (830 nm) to reject unwanted photons. Images were acquired and processed using WinView software from Princeton Instruments. Typically, an image of the animal was taken pre-administration of contrast agent. Subsequent images were taken post administration of the agent, all performed with the mouse in a stationary position. Data analysis consisted of subtracting (pixel by pixel) the pre-administration image from the post administration images, and displaying the results in false color.

Figure 4 shows that NIR fluorescently labeled MMG2 was retained in the tumor at 5 h postinjection. At 24 h, however, the probe completely cleared from blood and localized predominantly in the kidneys (ex-vivo image).

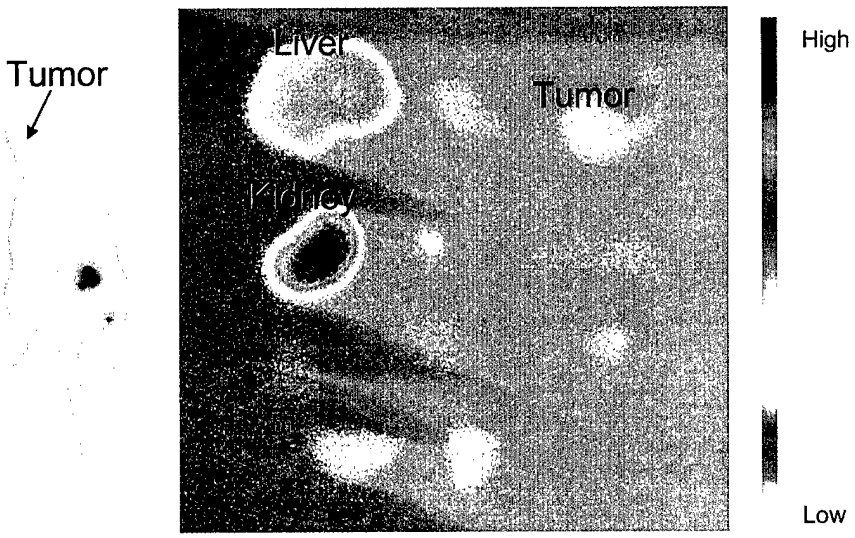

Figure 4: Distribution of Cypate MMG2 in a MDA-MB-361 tumor-bearing nude mouse. Whole body image (left panel) is at 5 h postinjection and organ parts (right panel) image was taken at 24 h postinjection.

Using the statistical package in WinView, we determined the relative accumulation of the probe in ex-vivo organ parts (Figure 5). The result shows that the selectivity of the probe for the tumor is not high relative to other organs. This could result from the small size of the tumor used, which was hardly palpable, or the probe may have low affinity for putative receptor on the surface of the tumor cells. It is also possible that MMG receptors are not present on the tumor surface. Alternatively, when compared with the good image obtained with the polyclonal antibody labeled near infrared probe, the result may indicate that the best approach to image the expression of MMG is to target its local concentration in the vicinity of the tumors by using anti-MMG antibody. These issues will be clarified with a fast growing MMG-positive tumor cell line.

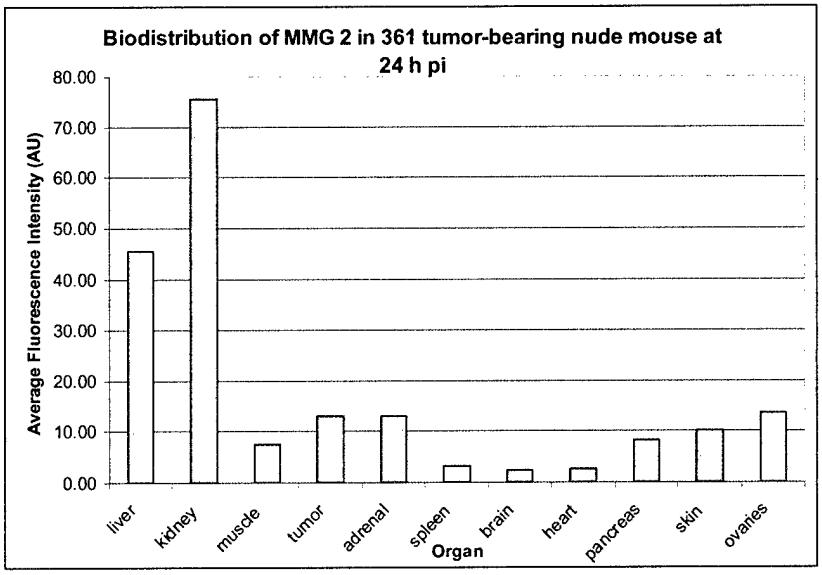

Figure 5: Ex-vivo distribution cypate MMG2 in MDA-MB-361 tumor-bearing nude mouse tissues. at 24 h postinjection.

A similar result described above was obtained with MMG3, except that this compound equally distributed in the liver and the kidneys (Figure 6). Tumor uptake was modest.

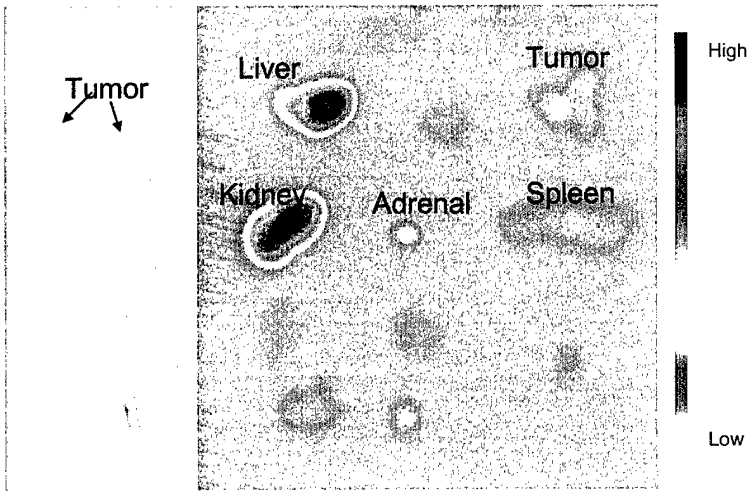

Figure 6: Distribution of Cypate MMG3 in a MDA-MB-361 tumor-bearing nude mouse. Whole body (left panel) and organ parts (right panel) images were taken at 24 h postinjection.

(ii) Radiolabeling of DOTA-MMG-Peptide and AMAB with ^{64}Cu and microPET imaging in MDA-MB-361 tumor-bearing mice

(a) Radiolabeling: The labeling of MMG2 peptide analogue is representative of the method used to prepare the radiopharmaceuticals for PET imaging studies.

Conjugation of the peptide with the chelating group (DOTA) was accomplished on solid support, as described in Task 1c. The peptide was dissolved in 480 µL of 0.1M NH_4CIT buffer (pH 7.5), giving a colorless clear solution at a concentration of 0.5 µg/µL. The stock solution was stored at -80 °C. To radiolabel the peptide, DOTA-MMG2 solution (10-µg or 5-µg) was diluted with the NH_4CIT buffer to 100 µL, to which ~2.5 mCi of ^{64}Cu in 20 µL of 0.1M NH_4CIT (pH 7.5) was added. The resulting solutions were incubated at 43 °C for 30-min (1000 rpm). The reaction mixture was transferred to a C18 SepPak cartridge pre-washed with 5 mL of ethanol, followed by 5 mL of water. The SepPak was washed with 5 mL of water and the product eluted with 1 mL of ethanol. Different fractions of the ethanol eluents were collected in three vials and characterized by HPLC equipped with UV and radioactivity detectors. Two of the vials were combined to give 264 µCi in ~ 400 µL. Quality control by HPLC showed that the DOTA-MMG2 was successfully labeled with ^{64}Cu and its radiochemical purity was nearly 100%.

(b) MicroPET imaging: MDA-MB-361 human breast cancer cells were injected into the mammary fat pad of female nude mice. The tumor growth was very slow and after >2 months, it was still difficult to obtain palpable tumor mass. The mice were used in this form for in vivo biodistribution of the probes by microPET. Two of the nude mice were injected with 100 µCi (150 µL) of the radiolabeled MMG2 peptide analogue per mouse. Images at 0.5, 1, 4, and 24 h pi were taken.

The microPET images of ^{64}Cu-DOTA-MMG2 are shown in Figure 7. Tumor was not visible at any time points. It is probably because the tumor was too small to be imaged, or the tumor targeting specificity of ^{64}Cu-DOTA-MMG-Peptide was low. At 30 min postinjection, both mice showed a hot bladder. This indicates that some of the ^{64}Cu-DOTA-MMG2 was excreted via kidneys. The activity also cleared via intestines, as shown in the images at 30 min and 4 h postinjection.

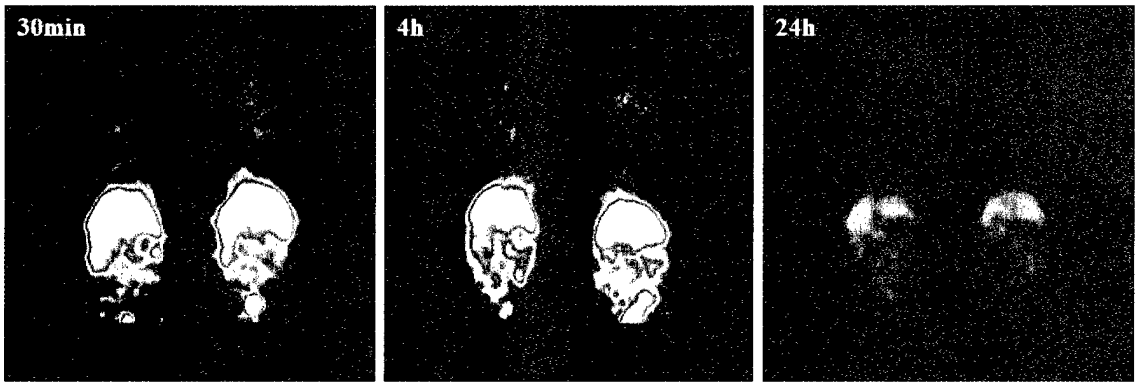

Figure 7: MicroPET coronal images of ^{64}Cu-DOTA-MMG2 in MC7-MAM tumor-bearing mice (n = 2). The image intensity is at the same scale.

The time-activity curves in visible organs are shown in Figure 8. It confirmed the observation that a significant amount of ^{64}Cu-DOTA-MMG2 was cleared via kidneys, which correlates with results of the optical imaging. Subsequently ex-vivo evaluation did not reveal the presence of the MMG-positive tumor in mice used for this study.

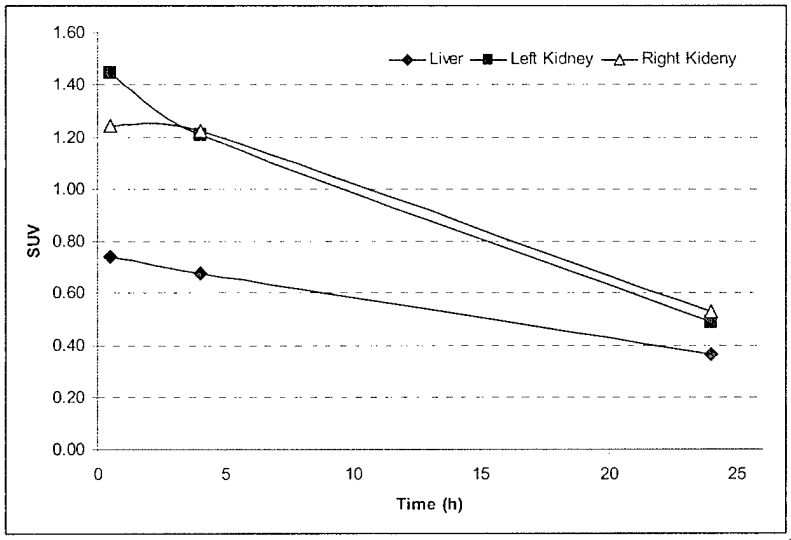

Figure 8: The time-activity curves from microPET imaging quantitative analysis of ^{64}Cu-DOTA-MMG-Peptide in MC7-MAM tumor-bearing mice.

A similar procedure for labeling and imaging MMG2 peptide analogue was used to evaluate the anti MMG monoclonal antibody developed for this study, except that the DOTA was first conjugated to the antibody by standard succinimidyl es-

ter activation mechanism. The microPET images of ^{64}Cu-DOTA-AMAB are shown in Figure 9.

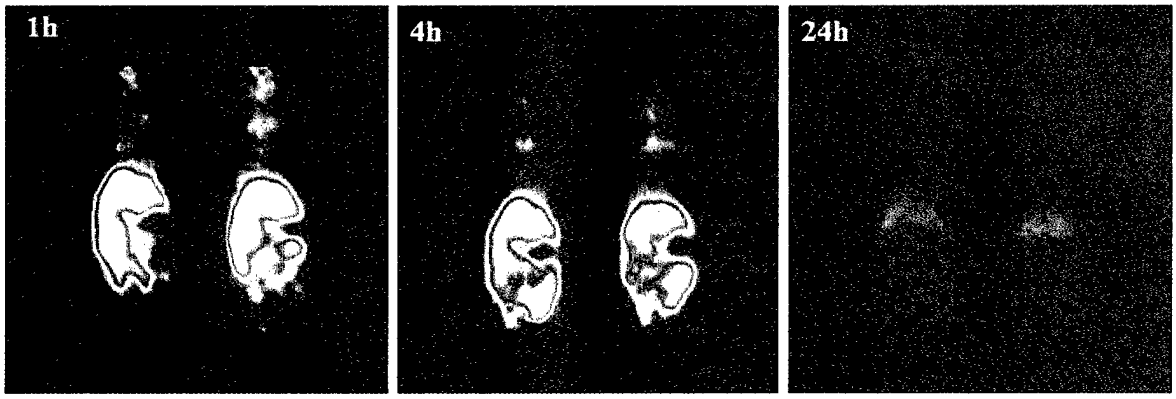

Figure 9: MicroPET coronal images of ^{64}Cu-DOTA-AMAB in MDA-MB-361 tumor-bearing mice (n = 2). The image intensity is on the same scale.

The time-activity curves in visible organs are shown in Figure 10. It appears that ^{64}Cu-DOTA-IgG was cleared via intestines.

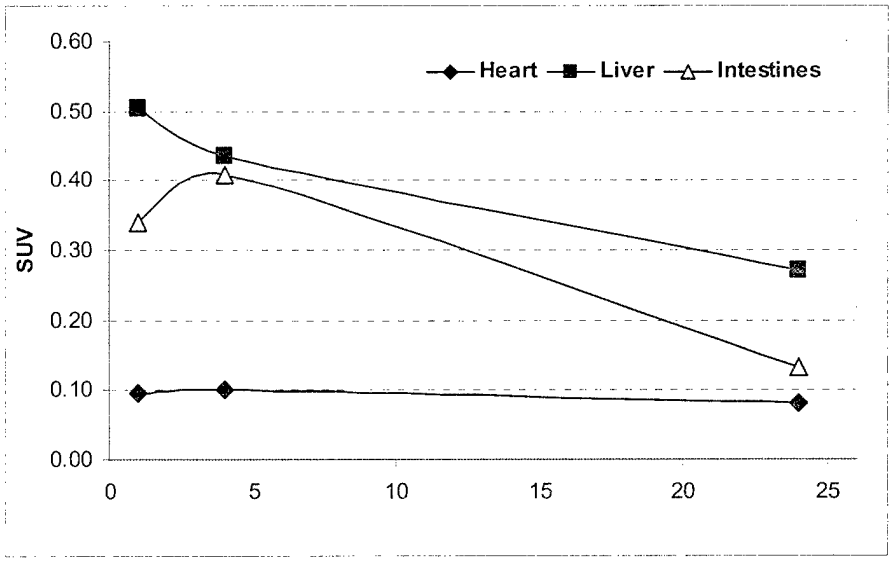

Figure 10: The time-activity curves from microPET imaging quantitative analysis of ^{64}Cu-DOTA-IgG in MDA-MB-361 tumor-bearing mice.

KEY RESEARCH ACCOMPLISHMENTS (2003-2004)

(1) We have prepared the first series of imaging agents for monitoring MMG expression by optical and nuclear methods.

(2) In vitro studies indicate that MMG may have anti-proliferative effect on breast cancer cells at > 1 μM concentrations. Interestingly, contrasting results were obtained with the MMG peptide fragments. While MMG3 appears to induce a concentration-independent proliferative effect, MMG2 was found to be neither cytotoxic nor induce cell proliferation.

(3) A Tat-MMG fusion protein has been developed and it will be used to probe intracellular MMG in MMG-positive cells.

(4) Optical and microPET imaging indicates that a suspected putative receptor for MMG may not be present on the tested MMG cell surfaces. Therefore, a preferred strategy to image MMG expression and, hence, detect breast cancers, is to develop and label molecules that bind to MMG with nuclear and optical probes. This is the focus of the final phase of this project.

REPORTABLE OUTCOMES

Presentations:

Invited Presentations:

1. S. Achilefu: The role of optical molecular probes in tumor imaging and organ function monitoring. Seminar Series, Intramural Research, National Institute of Child Health & Human Development, NIH, Bethesda, MD (December 8, 2003)

2. S. Achilefu: Lighting up tumors by optical methods. Roswell Cancer Institute Seminar, Buffalo, NY (December 1, 2003)

3. S. Achilefu: Contrast Agent-Mediated Optical Imaging of Tumors. Fall Meeting, American Association of Physicists in Medicine, Missouri River Valley Chapter, St. Louis, MO (November 8, 2003)

4. S. Achilefu: Receptor-specific near infrared molecular probes for imaging aberrant protein expression in vivo. *MGH Wellman Laboratories of Photomedicine Lecture Series*, Boston, MA (September 30, 2003)

5. S. Achilefu, Y. Ye, S. Bloch, R. Dorshow, K. Liang, T. Fleming: Near infrared molecular probes for imaging protein expression. *Imaging in 2020,* Jackson Hole, Wy (September 7-11, 2003)

6. S. Achilefu: Contrast agent-mediated organ function monitoring and tumor imaging by optical methods. *Advances in Optics for Biotechnology, Medicine and Surgery*, Banff, Alberta, Canada (August 3-7, 2003)

7. S. Achilefu, Y. Ye, S. Bloch: Diagnosis and treatment of tumors by optical methods. *The 31st Annual Meeting of the American Society for Photobiology*, Baltimore, MD (July 5-9, 2003)

8. S. Achilefu: Design of optical imaging agents. *NIH Workshop on Imaging the Pancreatic Beta Cells*, Bethesda, MD (April 21-22, 2003)

9. S. Achilefu: Imaging and monitoring therapeutic response of tumors by optical methods. *Washington University Small Animal Imaging Symposium*, St. Louis, MO (April 14, 2003)

10. S. Achilefu: Optical imaging – instrumentation and methods. *Siteman Cancer Center Oncologic Seminar Series*, Washington University Medical School, St. Louis, MO (December 9, 2002)

11. S. Achilefu: Optical contrast agent-mediated imaging of tumors. *Advanced Research Technologies Seminar Series*, Montreal, Canada (October 16, 2002)

12. S. Achilefu: Optical contrast agents for tumor imaging. *NIH Workshop on Optical Imaging*, Bethesda, MD (September 26-27, 2002)

13. S. Achilefu: Somatostatin beacon: a reliable model for targeted delivery. The *Society for Molecular Imaging Annual Meeting*, Boston, MA (August 26-27, 2002).

Other Presentations:

14. Z. Zhang, S. Achilefu: Synthesis and evaluation of polyhydroxylated near-infrared carbocyanine molecular probes. *International Symposium on Biomedical Optics*, SPIE, San Jose, CA (January 24-29, 2004).

Publications:

(1) Zhang, Z.; Achilefu, S. Synthesis and evaluation of polyhydroxylated near-infrared carbocyanine molecular probes. *Organic Letters* **2004 In Press**.
(2) Zhang, Z.; Bloch, S.; Achilefu, S. Synthesis and Evaluation of Novel Galactose-Carbocyanine Fluorescent Contrast Agents with Enhanced Hydrophilicity and Rigid Molecular Constraint. *Proc SPIE* **2004 In Press**, *4967*.
(3) Achilefu, S. Lighting up tumors with receptor-specific optical molecular probes. *Technology in Cancer Research & Treatment* **2004 In Press**.
(4) Achilefu, S. Optical Imaging Agents and Potential Application in the Assessment of Pancreatic Beta Cells. *Current Medicinal Chemistry - Immunology,Endocrine Metabolic Agents* **2004 In Press**.

CONCLUSIONS

In accordance with our stated goals in the first two years of this project, we have successfully demonstrated the potential to image the expression of MMG in MMG-positive tumors. Our results indicate that labeling molecules that bind MMG is a preferred strategy to image the expression of MMG in breast cancer than targeting putative cell surface MMG receptor.

REFERENCES

(1) Zhang, Z.; Achilefu, S. Synthesis and evaluation of polyhydroxylated near-infrared carbocyanine molecular probes. *Organic Letters* **2004 In Press**.
(2) Zhang, Z.; Bloch, S.; Achilefu, S. Synthesis and Evaluation of Novel Galactose-Carbocyanine Fluorescent Contrast Agents with Enhanced Hydrophilicity and Rigid Molecular Constraint. *Proc SPIE* **2004 In Press**, *4967*.
(3) Achilefu, S. Optical Imaging Agents and Potential Application in the Assessment of Pancreatic Beta Cells. *Current Medicinal Chemistry - Immunology,Endocrine Metabolic Agents* **2004 In Press**.
(4) Achilefu, S. Lighting up tumors with receptor-specific optical molecular probes. *Technology in Cancer Research & Treatment* **2004 In Press**.
(5) Achilefu, S.; Jimenez, H. N.; Dorshow, R. B.; Bugaj, J. E.; Webb, E. G. et al. Synthesis, in vitro receptor binding, and in vivo evaluation of fluorescein and carbocyanine peptide-based optical contrast agents. *Journal of Medicinal Chemistry* **2002**, *45*, 2003-2015.

(6) Achilefu, S.; Wilhelm, R. R.; Jimenez, H. N.; Schmidt, M. A.; Srinivasan, A. A new method for the synthesis of tri-tert-butyl diethylenetriaminepentaacetic acid and its derivatives. *Journal of Organic Chemistry* **2000**, *65*, 1562-1565.

(7) Atherton, E.; Sheppard, R. C. *Solid phase peptide synthesis: a practical appraoch*; Oxford University Press: Oxford, England, 1989.

(8) Achilefu, S.; Dorshow, R. B.; Bugaj, J. E.; Rajagopalan, R. Novel receptor-targeted fluorescent contrast agents for in vivo tumor imaging. *Investigative Radiology* **2000**, *35*, 479-485.

(9) Fanger, G. R.; Houghton, R. L.; Retter, M. W.; Hendrickson, R. C.; Babcook, J. et al. Detection of mammaglobin in the sera of patients with breast cancer. *Tumor Biology* **2002**, *23*, 212-221.

(10) Uray, I. P.; Liang, Y. Y.; Hyder, S. M. Estradiol down-regulates CD36 expression in human breast cancer cells. *Cancer Letters* **2004**, *207*, 101-107.

(11) Kudoh, M.; Knee, D. A.; Takayama, S.; Reed, J. C. Bag1 proteins regulate growth and survival of ZR-75-1 human breast cancer cells. *Cancer Research* **2002**, *62*, 1904-1909.

(12) Yin, J. J.; Mohammad, K. S.; Kakonen, S. M.; Harris, S.; Wu-Wong, J. R. et al. A causal role for endothelin-1 in the pathogenesis of osteoblastic bone metastases. *Proceedings of the National Academy of Sciences of the United States of America* **2003**, *100*, 10954-10959.

APPENDIX: Current Address Information

Current Address:

Samuel Achilefu, PhD
Associate Professor of Radiology
Department of Radiology
Washington University School of Medicine
Campus Box # 8225
4525 Scott Avenue - East Building
St. Louis, MO 63110-1093

Phone: 314 362 8599

Fax: 314 747 5191

E-mail: achilefus@mir.wustl.edu

ORGANIC LETTERS

XXXX
Vol. 0, No. 0
A–D

Synthesis and Evaluation of Polyhydroxylated Near-Infrared Carbocyanine Molecular Probes

Zongren Zhang and Samuel Achilefu*

Department of Radiology, Washington University, St. Louis, Missouri 63110

achilefus@wustl.edu

Received April 22, 2004

ABSTRACT

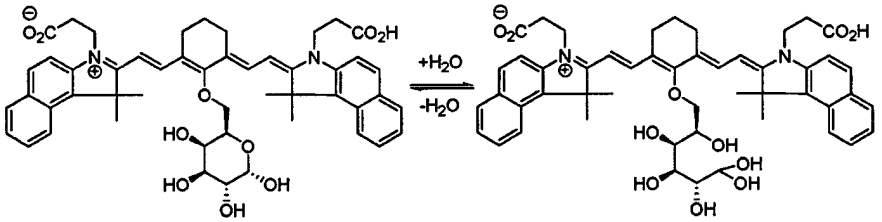

A new near-infrared (NIR) fluorescent molecular probe derived from indocarbocyanine dye and galactose was prepared, and the procedure was optimized. The presence of a nonionic polyhydroxyl moiety between hydrophobic groups enhances solubility and possibly minimizes aggregation in aqueous solutions. The structural framework of this molecule provides multivalent sites for labeling diverse molecules.

The resurgence of interest in detecting and imaging various diseases and analytes by optical methods has led to the development of methods for the synthesis and isolation of fluorescent probes in good yields and high purity.[1–4] Particularly, the use of carbocyanine (e.g., indocyanine green, ICG, Figure 1) and xanthene (e.g., fluorescein disodium salt) derivatives in humans shows that these fluorescent compounds are biocompatible, even at high concentrations of injected doses.[5] Because tissue autofluorescence and light absorption are low in the NIR wavelengths (750–900 nm), NIR light can travel several centimeters in heterogeneous systems such as cells and tissue phantoms. For this reason, molecular probes such as ICG and its reactive derivatives are useful for analyzing tissuelike heterogeneous samples by optical methods.[6,7]

The basic structural framework of many carbocyanine compounds consists of a linear polymethine unit that is flanked by symmetrical or nonsymmetrical aromatic groups.

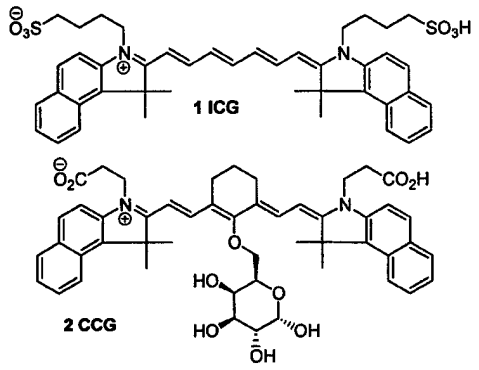

Figure 1. Structure of ICG and CCG.

(1) Achilefu, S.; Jimenez, H. N.; Dorshow, R. B.; Bugaj, J. E.; Webb, E. G.; Wilhelm, R. R.; Rajagopalan, R.; Johler, J.; Erion, J. L. *J. Med. Chem.* **2002**, *45*, 2003–2015.

(2) Pham, W.; Lai, W. F.; Weissleder, R.; Tung, C. H. *Bioconjugate Chem.* **2003**, *14*, 1048–1051.

(3) Mujumdar, R. B.; Ernst, L. A.; Mujumdar, S. R.; Lewis, C. J.; Waggoner, A. S. *Bioconjugate Chem.* **1993**, *4*, 105–111.

(4) Ye, Y.; Li, W. P.; Anderson, C. J.; Kao, J.; Nikiforovich, G. V.; Achilefu, S. *J. Am. Chem. Soc.* **2003**, *125*, 7766–7.

(5) Ntziachristos, V.; Yodh, A. G.; Schnall, M.; Chance, B. *Proc. Natl. Acad. Sci. U.S.A.* **2000**, *97*, 2767–2772.

10.1021/ol049258a CCC: $27.50
Published on Web 00/00/0000

Scheme 1

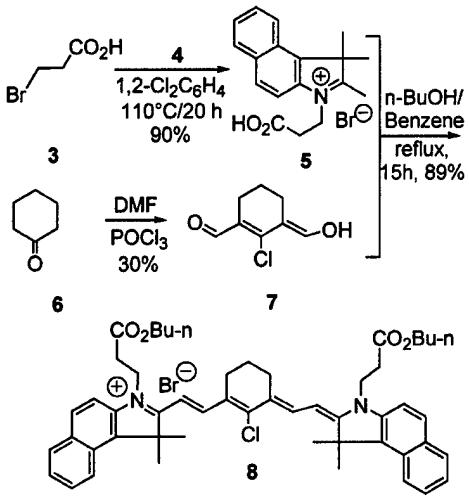

Scheme 2

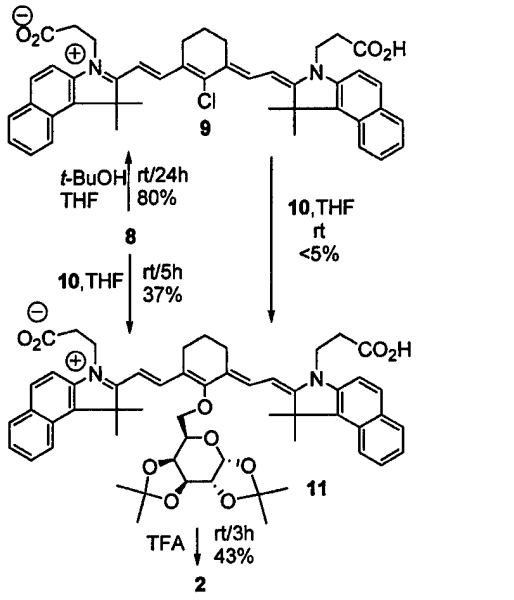

Predicated on previous findings that ICG derivatives that possess a conformationally constrained heptamethine moiety enhance fluorescence quantum yield and photochemical and photophysical stabilities of this class of compounds,[8,9] we designed and synthesized a novel NIR carbocyanine fluorescent probe containing galactose. The monosaccharide is incorporated in the central hydrophobic core of the chromophore system and anchored by ether linkage to the conformationally constrained cyclohexenyl group (CCG, **2**, Figure 1). Interestingly, the structural framework of the cyclohexenyl cypate-galactose **2** possesses multiple sites for homogeneous or heterogeneous labeling of biomolecules, drugs, and analytes with a single fluorescent molecule. Additionally, the nonionic polyhydroxyl group of galactose provides a mild hydrophilic environment for labeling molecules that are sensitive to the presence of strong anions such as the sulfonates used to improve water solubility in most carbocyanine molecular probes. CCG is also attractive because of the possibility of reducing aggregation of the probe in aqueous solutions.

The methods used to synthesize compound **2** are shown in Schemes 1 and 2. Reaction of 3-bromopropionic acid **3** with 2,3,3-trimethylbenzoindolenine **4** in 1,2-dichlorobenzene for 20 h at 120 °C gave the benzoindole carboxylic acid derivative **5** in 90% yield (Scheme 1). The intermediate **5** can be produced as needlelike crystals directly from the reaction mixture by controlled heating of the mixture between 100 and 105 °C in a cylindrical glass vessel. Synthesis of the second intermediate, 2-chloro-1-formyl-3-(hydroxymethylene)cyclohex-1-ene **7**, was performed by following a literature method.[10] We isolated **7** by H_2O/DCM extraction. The DCM phase was percolated through a $MgSO_4$ column, and the filtrate was concentrated on a rotary evaporator. Treatment of the residue with pentane gave the chloroaldehyde **7** as yellow crystalline solid. The chloraldehyde is not stable at room temperature and must be handled with care. For prolonged storage, **7** was converted to its stable aniline Schiff base.

In attempts to prepare chloro cylcohexenyl cypate (CCC, **9**, Scheme 2) from **7** and **5** using a literature method,[11] we obtained mixtures of **8**, **9**, and the mono-*n*-butyl ester. The ratios of these compounds varied under different reaction times and temperatures. For example, the proportion of CCC **9** in the mixture increased at lower temperatures and shorter reaction times relative to the conditions used to prepare **8**. The use of *n*-BuOH as a reaction solvent was beneficial in subsequent reactions under strongly basic conditions because it gave *n*-butyl esters of the carboxylic acid groups that served as a transient protecting group. Further optimization of the reaction conditions led selectively to the synthesis of **8** in excellent yield without base or acid catalysis. Evaluation of the reactivity of **7** and its aniline Schiff base derivatives (dianiline and dianiline monohydrochloride) showed that freshly prepared **7** gave excellent yield of the desired compounds compared with the aniline and aniline hydrochloride derivatives.

Etherification of **8** with galactose was accomplished by using 1,2,3,4-di-*O*-isopropylidene-D-galactopyranose (**10**) in freshly distilled THF. The solution was cooled to −78 °C, and a stoichiometric amount of *n*-BuLi was added to generate the reactive lithium alkoxide of D-galactopyranose. After

(6) Sevick-Muraca, E. M.; Houston, J. P.; Gurfinkel, M. *Curr. Opin. Chem. Biol.* **2002**, *6*, 642−650.
(7) Achilefu, S.; Dorshow, R. B.; Bugaj, J. E.; Rajagopalan, R. *Invest. Radiol.* **2000**, *35*, 479−485.
(8) Tarazi, L.; George, A.; Patonay, G.; Strekowski, L. *Talanta* **1998**, *46*, 1413−1424.
(9) Gorecki, T.; Patonay, G.; Strekowski, L.; Chin, R.; Salazar, N. *J. Heterocycl. Chem.* **1996**, *33*, 1871−1876.
(10) Reynolds, G. A.; Drexhage, K. H. *J. Org. Chem.* **1977**, *42*, 885−888.
(11) Narayanan, N.; Patonay, G. *J. Org. Chem.* **1995**, *60*, 2391−2395.

Scheme 3

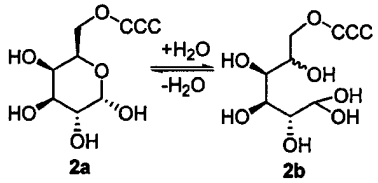

adding **8** in solid form, the reaction mixture was allowed to warm to room temperature. Interestingly, the alkaline reaction condition also removed the *n*-butyl ester to give isopropylidene-protected **11** in good yields (30−50%).[12] We observed that the best workup conditions for isolating **11** were obtained by (i) neutralizing the crude mixture, with HBr, (ii) evaporating the solvent, and (iii) washing the solid residue with water. Deprotection of the isopropylidene group of **11** with TFA at room temperature for 3 h gave the expected compound **2** in 43% yield as a green solid. The product was purified by reverse-column chromatography.

CCC **9** is an important NIR fluorescent compound that can be used to prepare dendritic arrays of dye-labeled molecules because of the availability of multiple reactive sites. We found that *n*-butyl-protected **8** can be effectively deprotected with THF/*t*-BuONa to give **9** in high yield (80%). Rapid precipitation of **9** from THF facilitates the reaction, and isolation of **9** and prevents its degradation in the basic reaction mixture (Scheme 2). However, attempts to prepare **11** from **9** gave a very low yield of the expected compound (<5%), even in the presence of excess lithium galactopyranose salt.

Although we were able to identify the cyclic analogue by MS, both **11** and **2** exist predominantly in the hydrated linear gem diol form (Scheme 3).

Shown in Figure 2 are the absorption and fluorescence spectra of **2**, which is representative of the spectral properties of the new molecular probes prepared. All the compounds have similar absorption and fluorescence emission maxima in 20% aqueous DMSO. This indicates that direct substitution of the chloro group with an alkoxyl group at the central hydrophobic chromophore system had negligible effects on the spectral properties of the compounds. The small Stokes shift of <15 nm observed is typical of many NIR cyanine fluorescent probes. However, the absorption spectrum is broad, enabling excitation of the molecule at any wavelength between 650 and 810 nm. For example, exciting the probe at 750 nm and monitoring the fluorescence emission at 825 nm would minimize the challenge of rejecting stray excitation light by the emission filter.

Cyanine dyes are known to aggregate in aqueous solutions because of the structural arrangement of their hydrophobic core.[13,14] The aggregates affect dye solubility and optical properties. A common aggregation mode in cyanine dyes is *J*-aggregates, which are polymerlike stackings of molecules

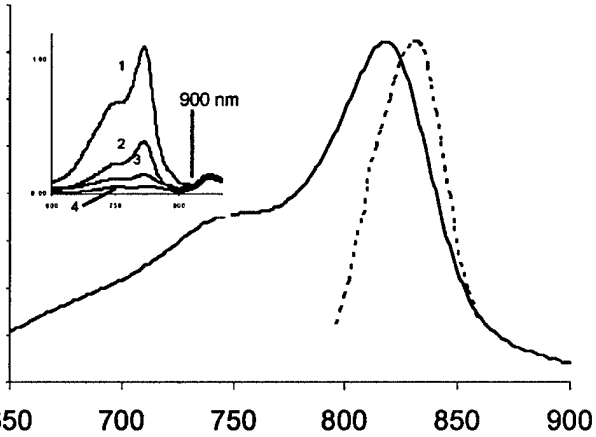

Figure 2. Absorption (solid line) and fluorescence (dashed line) spectra of **2** in 20% aqueous DMSO solution. *y*-Axis: Normalized absorption and fluorescence intensity in arbitrary unit. *x*-Axis: wavelength in nm. Inset: Absorption spectra of **2** at different concentrations (**1**, 3.0×10^{-6} M; **2**, 7.5×10^{-7} M; **3**, 1.9×10^{-7} M; **4**, 4.7×10^{-8} M). Peaks >900 nm are nearly unchanged.

in aqueous solvents. Spectroscopically, the *J*-aggregates are manifested by a new sharp absorption band at longer wavelengths with respect to the major long-wavelength absorption of monomers.[15] The small bumps at 972 nm observed in the absorption spectrum of **2** (Figure 2, insert) at different concentrations probably correspond to *J*-aggregates. This is similar to what was observed in the absorption spectrum of benzimidazolocarbocyanine.[15] The peak does not show noticeable increases in intensity at higher concentrations, and it is not as sharp as the *J*-aggregates band of benzimidazolocarbocyanine. We compared the aggregation pattern of **2** with the hydrophobic **8**. The results show that **8**, which is more susceptible to forming aggregates than **2**, has a small secondary absorption peak at 896 nm, possibly arising from *J*-aggregates. At the same molar concentration (3.0 μM), this peak is nearly 5 times more intense than that of compound **2** at 972 nm. Thus, the new molecular design may have reduced aggregate formation in aqueous medium.

Our preliminary results of the in vivo distribution of **2** in normal nude mice showed that **2** rapidly clears from blood and is predominately excreted by the hepatobiliary system within 5 min postinjection. The fast clearance from blood reduces background fluorescence, thereby enabling rapid visualization of target tissue.

In conclusion, we have synthesized a new conformationally constrained NIR fluorescent probe with enhanced water solubility and biocompatibility. The presence of a structurally constrained cyclic substructure, a nonionic polyhydroxyl moiety, and multiple reactive functional groups makes **2** a robust molecular probe for a variety of chemical and

(12) Strekowski, L.; Lipowska, M.; Patonay, G. *J. Org. Chem.* **1992**, *57*, 4578−4580.

(13) Khairutdinov, R. F.; Serpone, N. *J. Phys. Chem. B* **1997**, *101*, 2602−2610.

(14) Reers, M.; Smith, T. W.; Chen, L. B. *Biochemistry* **1991**, *30*, 4480−4486.

(15) Egorov, V. V. *J. Chem. Phys.* **2002**, *116*, 3090−3103.

biological applications. We are currently exploring the use of this compound to study diseased tissue by optical methods.

Acknowledgment. This study was funded in part by research grants from the NSF (BES 0119489), Siteman Cancer Center Research Development Award and the US Army breast cancer research award (DAMD17-02-1-0613). We thank Sharon Bloch for biodistribution studies.

Supporting Information Available: Experimental procedures for all compounds, characterization for key compounds, and description and results of biodistribution studies. This material is available free of charge via the Internet at http://pubs.acs.org.

OL049258A

Synthesis and Evaluation of Novel Galactose-Carbocyanine Fluorescent Contrast Agents with Enhanced Hydrophilicity and Rigid Molecular Constraint

Zongren Zhang, Sharon Bloch, and Samuel Achilefu*
Department of Radiology, Washington University, St. Louis, Missouri 63110

ABSTRACT

A new carbocyanine optical molecular probe with enhanced water solubility and constrained structural conformations was designed and synthesized. The near infrared (NIR) fluorescent probe contains a nonionic D-galactopyranose, which could improve water solubility of the probe and enhance uptake in tumors mediated by glucose transporter. The possibility of multiple attachment points provides the potential to conjugate diverse bioactive molecules to the probe. We developed an efficient synthetic method that is optimized for large-scale synthesis. Preliminary in vivo biodistribution studies show that the probe is rapidly cleared from blood and localize in the liver as early as 5 minutes post-injection of the probe in nude mice. Additional studies to evaluate the tumor uptake of the probe and its bioactive peptide conjugates are in progress.

Keywords: Hydrophilic carbocyanine, galactose, glucose, near infrared contrast agent, synthesis, tumor, fluorescent dye, molecular probe, aggregate.

1. INTRODUCTION

Biomedical optical imaging is one of the fast growing areas of biomedical research because of its high sensitivity that approaches that of nuclear methods without the use of ionizing radiation. A further attraction of this emerging technology is the potential to develop cost-effective imaging systems for medical applications and the possibility of monitoring molecular processes with exogenous contrast agents. The propagation of light in tissue is wavelength dependent. For this reason, optical imaging in the visible wavelengths is conventionally used to evaluate superficial lesions, endoscope-accessible deep organs, and surgically exposed tissues because of the shallow penetration of light in this region. This light attenuation is due to endogenous absorption and scattering biomolecules and cell organelles. At the NIR region between 700 and 900 nm, absorption by intrinsic photoactive biomolecules is low, allowing light to penetrate several centimeters into tissues, a feature that is useful for imaging diseases in deep tissues.

Presently, fluorescein, indocyanine green (ICG, Figure 1) and fluorescent photosensitizers are widely used as optical molecular probes for in vivo imaging of tumors, possibly due to their established safety profile in humans and known photophysical properties.[1-6] Of these classes of compounds, carbocyanine dyes are the most widely used NIR optical probes for imaging tumors in small animals and humans because of their high molar absorptivity in organic and aqueous solvents.[7-11] The basic structural framework of carbocyanine dyes consists of a highly conjugated methine group that is flanked by symmetrical or nonsymmetrical aromatic groups (Figure 1). While ICG has been used for numerous contrast agent-mediated optical imaging studies, it does not have functional groups for covalently bonding to bioactive molecules. Consequently, several derivatives of ICG have been developed to overcome this problem.[7, 12-16] One of these probes (Cypate, Figure 1) have been shown to have similar spectral properties and blood clearance profile in rodents as ICG.[7]

Predicated on the pioneering work of Patonay's group,[17, 18] which showed that the fluorescence quantum yield and photophysical stability of NIR carbocyanines can be enhanced by rigidifying the flexible heptamethine group of ICG, we designed and synthesized a novel carbohydrate-based NIR carbocyanine fluorescent probe. The new molecular construct is expected to have several advantages over currently available probes. Some of these include the use of nonionic hydrophilic group to increase water solubility of the probe, the use of glucose derivatives to enhance selective retention

* achilefus@wustl.edu; phone 1 314 362-8599; fax 1 314 747-5191

of the probe in hypermetabolizing tumors through glucose transporters, availability of multiple functional groups for possible conjugation of biomolecules and drugs, and the possibility of reducing aggregation of the probe in aqueous solutions by incorporating a conformationally constrained cyclic structure into the heptamethine unit of cypate. The resulting design, chloro cyclic cypate (CCC)-galactose is shown in Figure 1.

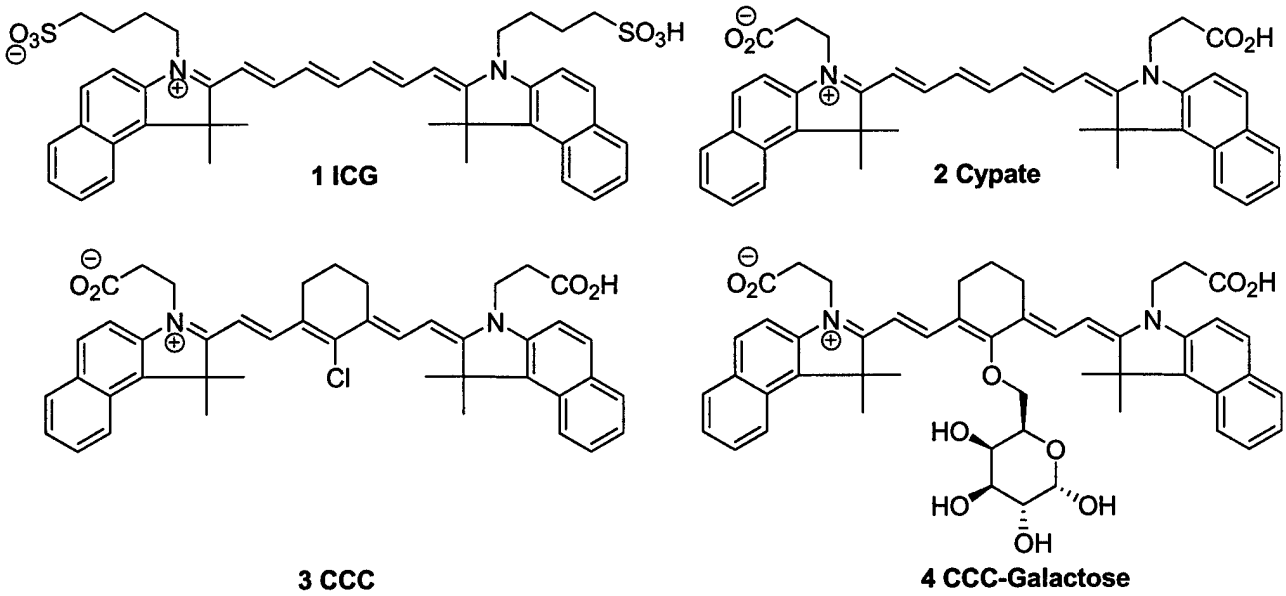

Fig1. Structure comparison of ICG, cypate, CCC and CCC-galactose

2. SYNTHESIS

Carbocyanine dyes are usually made by condensation of a conjugated dialdehyde derivative and aromatic heterocylic compounds containing active protons. Starting with 2-chloro-1-formyl-3-(hydroxymethylene)cyclohex-1-ene **8** (Scheme 1), we simultaneously introduced a cyclohexenyl group and a reactive chloro substituent between the benzoindole groups of cypate to give intermediate CCC derivatives **9**. Further reaction of **9** with galactose gave the desired compound. Interestingly, CCC (Figure 1) that was isolated from syntheses of protected CCC **9** under nonselective conditions, is a versatile fluorescent dye that can be used as a platform to synthesize a variety of molecular probes for biomedical optical imaging applications.

Initial attempts to synthesize CCC-galactose by protecting the carboxyl group with *t*-butyl group following a method reported in the literature gave the compound in low yields.[19] Considering that the carboxylic acid group might not interfere with the etherification of the chlorinated dye intermediate when excess nucleophilic carbohydrate is used, we simplified the synthetic procedure, as shown in Scheme 1. The new procedure led to the efficient synthesis of CCC-galactose **4** in a good yield.

3-Bromopropionic acid **6** reacted with 2,3,3-trimethylbenzoindolenine **5** to give indole acid **7** after stirring the two in 1,2-dichlorobezene for 20 h at 100°C. 2-Chloro-1-formyl-3-(hydroxymethylene)cyclohex-1-ene **8** was synthesized following a literature method.[20] We isolated **8** by extraction with DCM/H_2O mixture. Surprisingly, reaction of **7** with the aldehyde **8** in *n*-BuOH/benzene (8/2) led directly to n-butyl protected CCC **9** selectively in most cases instead of the expected CCC. We also studied the synthesis of CCC with different forms the aldehyde **8**. Excellent yield was achieved when the aldehyde **8** was freshly prepared as compared with the syntheses from the same compound in storage. Similarly, poor yields were obtained with aniline-protected Schiff bases of **8**. Using excess 1,2,3,4-di-*O*-isopropylidene-D-galactopyranose, deprotonated with stoichiometric *n*-BuLi at –78°C in THF, acetonide protected CCC-galactose **11** was produced in moderate (30-50%) yield. Removal of protective n-butyl group was achieved simultaneously under this

alkaline condition. The excess galactose present in the reaction mixture was removed prior to HPLC separation by repeatedly washing the reaction residue with water after neutralization with diluted HCl and solvent removal. Deprotection of **11** in TFA at room temperature in 3 h gave the expected CCC-galactose **4** in 43% yield as a green solid. Although dye intermediates can usually be made in moderate purity via extraction using DCM/H_2O mixture, important dyes and dye intermediates were purified by chromatography. For compounds **11** and **4**, reverse HPLC column with aqueous eluents was used because of the nature of carbohydrate chemistry.

Scheme 1

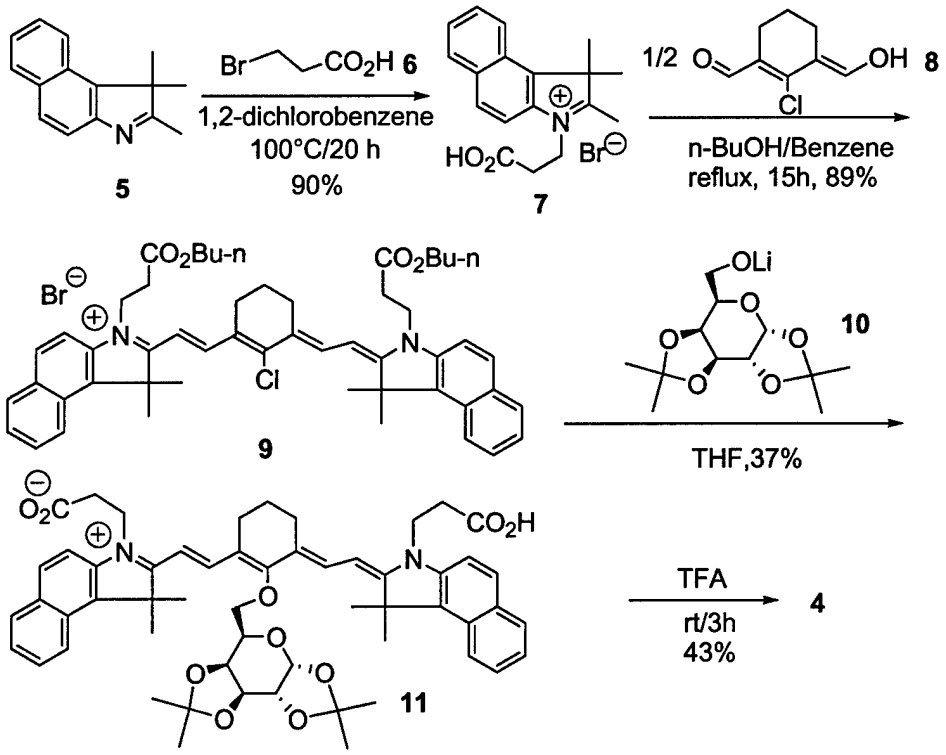

3. CHEMICAL AND PHOTOPHYSICAL PROPERTIES

Hydrophilicity is an important consideration in developing novel fluorescent contrast agents for biomedical optical imaging. Clear differences in the solubility of the few dyes prepared were observed. Similar to cypate, non-sugar modified CCC is hydrophobic even in the presence of two carboxylic acid groups. When protected with n-butyl, the compound **9** is readily soluble in organic solvents while CCC and acetonide protected CCC-galactose **11** are more soluble in polar organic solvents. Compound **11** showed some hydrophilic tendency even in its protected form. It is soluble in aqueous solvents in the presence of polar organic solvents. The final dye molecule, CCC-galactose **4**, is noticeably hydrophilic. For example, a small amount of MeOH would move CCC-galactose **4** from DCM layer to water layer while acetonide protected CCC-galactose **11** remained in DCM layer even at significantly increased MeOH content.

CCC showed maximum absorbance peak at 818 nm in 20% DSMO in water. Modification with galactose molecule did not alter the absorption spectrum, however, slight bathochromic shift was observed from the *n*-butyl ester derivative **9**. This indicates that direct substitution with alkoxyl group at the middle of the conjugated chromophore system did not affect the absorption spectral properties of the chromophore. Their fluorescence emission behaves similarly, with small Stokes shift of <15 nm. This is typical of most NIR cyanine dyes. Shown in Fig. 2 are the absorption and fluorescence

spectra of CCC-galactose **4**, which is representative of the spectral properties of the series of the new molecular probes prepared.

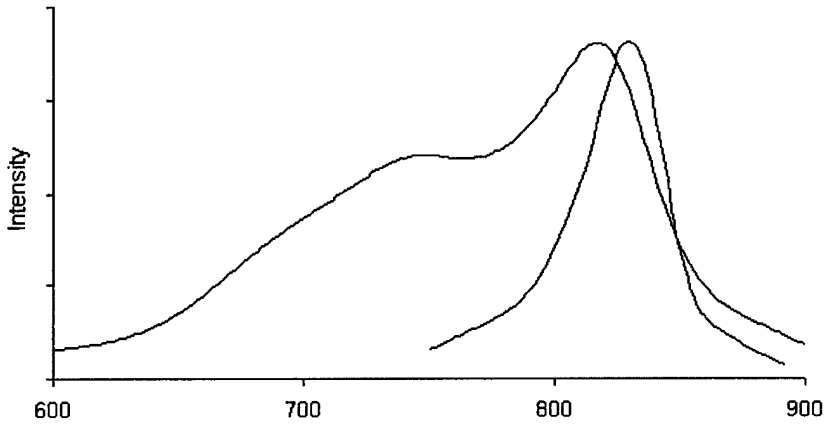

Fig 2 Absorption and fluorescence spectra of CCC-galactose **4** in 20% aqueous DMSO

Carbocyanine dyes are known to aggregate in aqueous solutions because of the structural arrangement of the hydrophobic core of the molecules. These aggregates arise from supramolecular assembly in aqueous media, which influences the optical properties of dyes.[17] A common supramolecular assembly in cyanine dyes are *J*-aggregates, which are polymer-like stacking of dye molecules in aqueous solvents. The formation of the assembly is believed to be driven by enthalpy and the attractive interaction of π-electrons of the planar chromospheres of the dye molecules.[21] Spectroscopically, the *J*-aggregates are manifested by a new sharp absorption band at longer wavelengths with respect to the major absorption long-wavelength of monomers.[22] The small bump at 972 nm in the absorption spectrum of CCC-galactose **4** probably corresponds to *J*-aggregates (Figure 3), which is similar to what was observed in the absorption spectrum of benzimidazolocarbocyanine.[22] The peak does not show noticeable increase in intensity at high concentrations and it is not as sharp as *J*-aggregates band of benzimidazolocarbocyanine. Thus, the new molecular design may have reduced aggregate formation in aqueous medium.

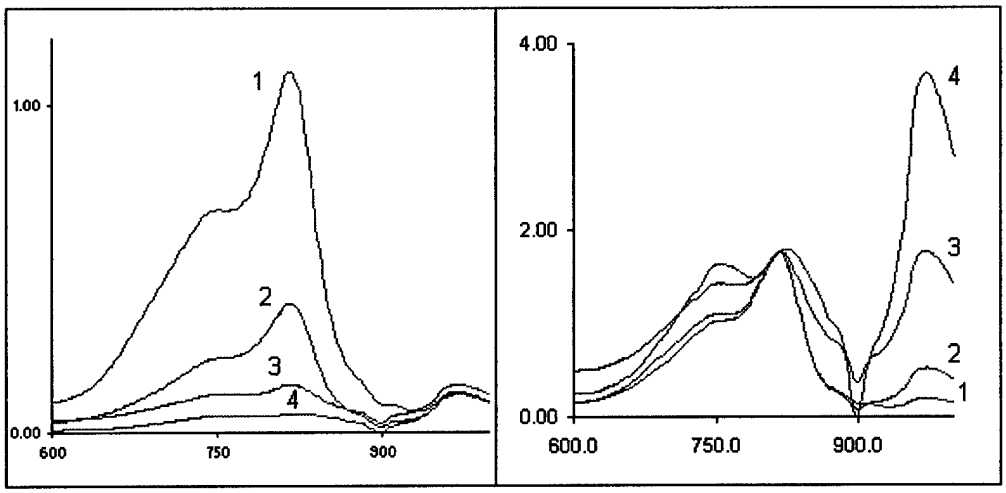

Fig. 3. UV absorptions of CCC-galactose **4** at different concentrations (left) and its normalized display (right) in 20% aqueous DMSO) (1: $3.0X10^{-6}$ M, 2: $7.5X10^{-7}$ M, 3: $1.9X10^{-7}$ M, 4: $4.7X10^{-8}$ M); X-axis: Wavelength (nm), Y-axis: Absorption.

4. BIODISTRIBUTION OF CCC-GALACTOSE IN NUDE MICE

Optical projection imaging is a simple method to rapidly evaluate the distribution of optical molecular probes in rodents. The optical imager is not expensive and its operation is not complicated. Typically, the instrument consists of an excitation source and a charge-coupled device (CCD) camera for signal detection. We employed a nominal 780 nm collimated solid state laser source to excite CCC-galactose **4**. The nominal 50 mW of incident power was reduced to about 20 mW at the output of the fiber optic bundle. A CCD camera (12 bit, 1024 x 1024 pixel, back illuminated) was equipped with the appropriate interference filter to capture the emitted photons at 830 nm. All animal experiments were preformed in accordance with the Washington University Protocol for the use of laboratory animals. Nude mice were anaesthetized and injected with a 100 μL of a 60 μM solution of CCC-galactose **4**. Time-sequence images of the mice were performed and the rodents were sacrificed at 24 h post-injection of the probes. Our results indicate that CCC-galactose **4** was predominantly excreted by the hepatobiliary system within 5 minutes post-injection. This excretion rate appears to be much faster than ICG and cypate, whose localization in live rodents observed by planar optical imaging is typically between 30 and 60 minutes post-injection. Figure 4 shows the time-sequence imaging and ex-vivo biodistribution in normal nude mice. The ex-vivo biodistribution was obtained after the animal was sacrificed at 24 h post-injection of the probe.

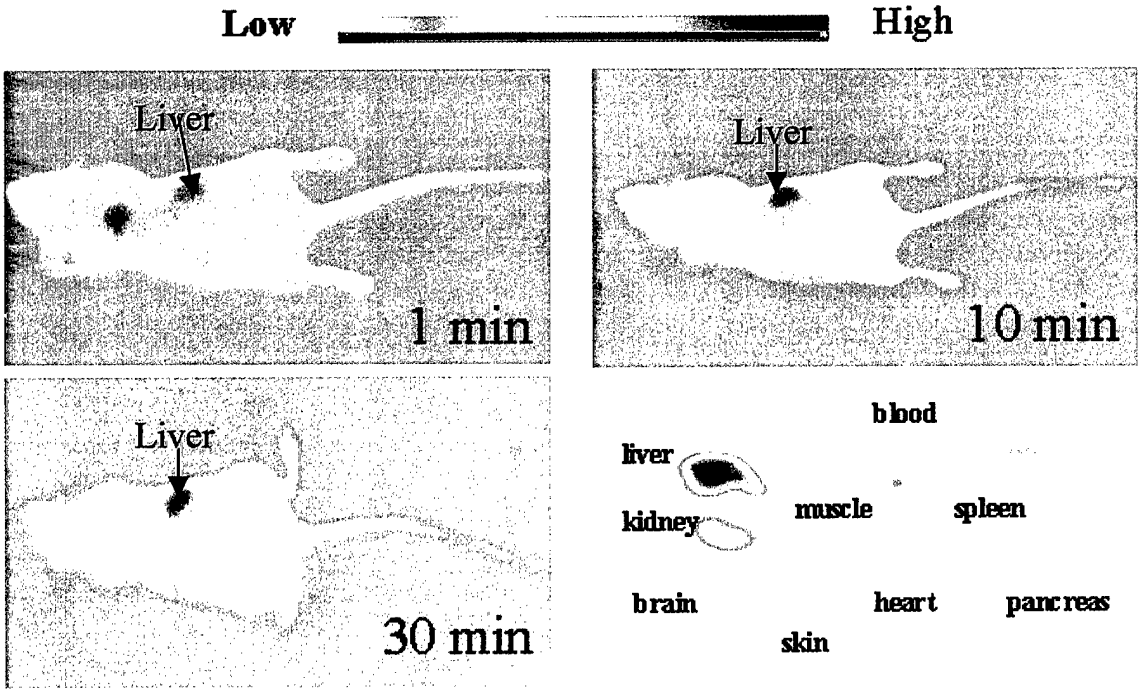

Fig. 4. Time sequence imaging of the biodistribution of CCC-galactose in nude mice. Oran parts were images ex-vivo at 24 h post-injection of the probe

5. MATERIALS AND METHODS

General. Reagents and solvents were purchased from commercial source. THF used in the galactose derivatization was distilled after refluxing in sodium for two days. Reactions were usually monitored by either HPLC with UV monitor or TLC with visual observation of the dye spots. In most cases, product purification was performed by silica gel column, C-18 reverse silica gel column and semipreparative HPLC until a single HPLC peak and single MS peak were produced. Mass spectra were provided by The Protein Chemistry Laboratory at Washington University. Absorption spectra were

recorded on Beckman Coulter DU 640 UV-Vis spectrometer. Fluorescent emission spectra were recorded on a Jobin Yvon-Spex Fluorolog-3 spectrofluorometer.

1-Carboxyethyl-2,3,3-trimethylbenzoindoleninium bromide (7). 2,3,3-Trimethylbenzoindolenine (5.81 g, 27.8 mmol) and 3-bromopropionic acid (4.23 g, 27.7 mmol) were dissolved in 1,2-dichlorobenzene (80 mL). The mixture was stirred at 100 °C for 20 h leading to crystalline precipitate. The mixture was cooled to room temperature. Products were filtered, washed with ether and dried to give 9.0 g (90%) of **7** as slightly colored crystals. ^{1}H NMR (DMSO, 300 MHz): δ 8.36 (d, *J*=8.4 Hz, 1H), 8.28 (d, *J*=10.8 Hz, 1H), 8.22 (d, *J*=8.4 Hz, 1H), 8.16 (d, *J*=10.8 Hz, 1H), 7.78-7.72(m, 2H), 4.77 (t, *J*= 6.9Hz, 2H), 3.52 (br, 1H), 3.04 (t, *J*= 6.9Hz, 2H), 2.97 (s, 3H), 1.75 (s, 6H).

2-Chloro-1-formyl-3-(hydroxymethylene)cyclohex-1-ene (8). A solution of $POCl_3$ (37 mL, 397 mmol) in DCM (35 mL) was added to an ice-cooled solution of DMF (40 mL, 516 mmol) in DCM (40 mL) slowly while the latter was stirred. After adding the $POCl_3$, cyclohexanone (10 g, 100 mmol) was added to the reaction mixture via a syringe. The resulting reaction mixture was refluxed for 2 h. The mixture was then cooled in ice. Water (200 mL), pre-cooled to 0°C was added. The mixture was stirred for 30 min. DCM layer was saved. Aqueous layer was extracted with additional DCM. The DCM solutions were combined, passed through a $MgSO_4$ column, concentrated on a rotary evaporator and treated with pentane (200 mL) to give 4.68 g (27%) of **8** as yellow crystalline solid. Partial aldehyde **8** was converted to its stable aniline Schiff base by adding aniline to its saturated ether solution, and to its Schiff base monohydrochloride by adding concentrated HCl to the saturated DCM solution of its Schiff base.

n-Butyl protected CCC (9). Into a flask attached with Dean-Stark trap and a condenser were added 1-carboxyethyl-2,3,3-trimethylbenzoindoleninium bromide **7** (14.43 g, 39.83 mmol), freshly prepared 2-chloro-1-formyl-3-(hydroxymethylene)cyclohex-1-ene **8** (3.42 g, 20 mmol), *n*-butanol (300 mL) and benzene (30 mL). The mixture was refluxed for 4 h to give a green solution. Solvents were removed on a rotavapor. Residue was washed with hexane/EtOAc and eluted with DCM/MeOH from a silica gel plug to give crude product as dark green solid. Further chromatography on a silica gel column with gradient Hexane/EtOAc-DCM/MeOH system gave 12.4 g (89%) of **9** as dark green solid. MS/EI: 811(100) (M^+).

Acetonide protected CCC-galactose (11). Into an argon-flushed, dry ice-cooled flask were added 1,2,3,4-di-*O*-isopropylidene-D-galactopyranose (1.01 g, 3.89 mmol) and THF (anhydrous, 20 mL). The flask was then sealed with rubber septum and *t*-BuLi (1.7 M in pentane, 2.3 mL, 3.90 mmol) was added via a syringe. The resulting mixture was stirred for additional 30 min and was then transferred into a dry ice-cooled THF (20 mL) solution of n-butyl protected CCC **9** (0.6053 g, 0.87 mmol). The mixture was then stirred for 5 h at room temperature and neutralize with hydrobromic acid. THF was removed and the residue was washed with water and dried over $MgSO_4$. The resulting dark green crude product was purified by chromatography on a C-18 silica gel column with water/MeCN as eluent to give 0.30 g (37%) of **11** as dark green solid. Further purification was made on preparative HPLC. MS/EI: 941(100) (M^++H_2O).

CCC-galactose (4). A trifluoroacetic acid (10 mL) solution of acetonide protected CCC-galactose **11** (57 mg, 60 μmol) was stirred at room temperature for 3 h. TFA was then removed by gently passing air through the reaction vessel. Residue was purified with preparative HPLC to give 22 mg (43%) of **4** as dark green solid. MS/EI: 861(100) (M^++H_2O).

6. CONCLUSION

We have synthesized a new galactose-carbocyanine optical molecular probe with increased water solubility and constrained conformation. The new probes absorb and emit radiation in the NIR wavelengths and the structural disposition makes it possible to conjugate it with diverse bioactive molecules. These studies are in progress for the imaging of tumors in rodents.

ACKNOWLEDGEMENT

This study was funded in part by research grants from the NSF (BES 0119489), Siteman Cancer Center Research Development Award and the US Army breast cancer research award (DAMD17-02-1-0613).

REFERENCES

1. Arsene S, Giraudeau B, Le Lez ML, Pisella PJ, Pourcelot L, Tranquart F., "Follow up by colour Doppler imaging of 102 patients with retinal vein occlusion over 1 year", *Br. J. Ophthalmol.,* **86,** 1243-1247, 2002.
2. Kaiser RS, Berger JW, Williams GA, et al., "Variability in fluorescein angiography interpretation for photodynamic therapy in age-related macular degeneration", *Retin.-J. Retin. Vitr. Dis.,* **22,** 683-690, 2002.
3. Pflugfelder SC, Solomon A, Stern ME., "The diagnosis and management of dry eye - A twenty-five-year review", *Cornea,* **19,** 644-649, 2002.
4. Raabe A, Beck J, Gerlach R, Zimmermann M, Seifert V., "Near-infrared indocyanine green video angiography: A new method for intraoperative assessment of vascular flow", *Neurosurgery,* **52,** 132-139, 2003.
5. Shaikh S, Ruby AJ, Williams GA., "Photodynamic therapy using verteporfin for choroidal neovascularization in angioid streaks", *Am. J. Ophthalmol.,* **135,** 1-6, 2003.
6. Tsilou E, Csaky K, Rubin BI, Gahl W, Kaiser-Kupfer M., "Retinal visualization in an eye with corneal crystals using indocyanine green videoangiography", *Am. J. Ophthalmol.,* **134,** 123-125, 2002.
7. Achilefu S, Dorshow RB, Bugaj JE, Rajagopalan R., "Novel receptor-targeted fluorescent contrast agents for in vivo tumor imaging", *Invest. Radiol.,* **35,** 479-485, 2000.
8. Gurfinkel M, Thompson AB, Ralston W, et al. "Pharmacokinetics of ICG and HPPH-car for the detection of normal and tumor tissue using fluorescence, near-infrared reflectance imaging: A case study", *Photochem. Photobiol.,* **72,** 94-102, 2000.
9. Ntziachristos V, Yodh AG, Schnall M, Chance B. "Concurrent MRI and diffuse optical tomography of breast after indocyanine green enhancement", *Proc. Natl. Acad. Sci. U. S. A.,* **97,** 2767-2772, 2000.
10. Intes X, Ripoll J, Chen Y, Nioka S, Yodh AG, Chance B., "In vivo continuous-wave optical breast imaging enhanced with Indocyanine Green", *Med. Phys.,* **30,** 1039-1047, 2003.
11. Malicka J, Gryczynski I, Geddes CD, Lakowicz JR., "Metal-enhanced emission from indocyanine green: a new approach to in vivo imaging", *J. Biomed. Op.,* **8,** 472-478, 2003.
12. Mujumdar RB, Ernst LA, Mujumdar SR, Lewis CJ, Waggoner AS., "Cyanine Dye Labeling Reagents - Sulfoindocyanine Succinimidyl Esters", *Bioconjugate Chem.,* **4,** 105-111, 1993.
13. Ballou B, Fisher GW, Waggoner AS, et al., "Tumor Labeling in-Vivo Using Cyanine-Conjugated Monoclonal-Antibodies", *Cancer Immunol. Immunother.,* **41,** 257-263, 1995.
14. Hirata T, Kogiso H, Morimoto K, et al., "Synthesis and reactivities of 3-indocyanine-green-acyl-1,3-thiazolidine-2-thione (ICG-ATT) as a new near-infrared fluorescent-labeling reagent", *Bioorg. Med. Chem.,* **6,** 2179-2184, 1998.
15. Lin YH, Weissleder R, Tung CH., Novel near-infrared cyanine fluorochromes: Synthesis, properties, and bioconjugation. *Bioconjugate Chem.* **13,** 605-610, 2002.
16. Pham W, Lai WF, Weissleder R, Tung CH., "High efficiency synthesis of a bioconjugatable near-infrared fluorochrome", *Bioconjugate Chem.,* **14,** 1048-1051, 2003.
17. Tarazi L, George A, Patonay G, Strekowski L., "Spectral characterization of a novel near-infrared cyanine dye: a study of its complexation with metal ions", *Talanta,* **46,** 1413-1424, 1998.
18. Gorecki T, Patonay G, Strekowski L, Chin R, Salazar N., "Synthesis of novel near-infrared cyanine dyes for metal ion determination", *J. Heterocycl. Chem,.* **33,** 1871-1876, 1996.
19 Narayanan, N.; Patonay, G., "A new method for the synthesis of heptamethine cyanine dyes: synthesis of new near-infrared fluorescent labels", *J. Org. Chem.*, **60,** 2391, 1995.
20 Reynolds GA; Drexhage KH., "Stable heptamethine pyrylium dyes that absorb in the infrared", *J. Org. Chem.,* **42(5),** 885-888, 1977.
21 Kobayashi, T., Ed. *J-aggregates*; World Scientific, Singapore, 1996.
22 Egorov, V. V., "Nature of the optical transition in polymethine dyes and J-aggregates", *J. Chem. Phys.,* **116,** 3090-3103, 2002.